ChemComm

COMMUNICATION

View Article Online
View Journal | View Issue

Cite this: *Chem. Commun.*, 2019, **55**, 11794

Received 22nd July 2019,
Accepted 6th September 2019

DOI: 10.1039/c9cc05659a

rsc.li/chemcomm

Comparative performance of Cu-zeolites in the isothermal conversion of methane to methanol†

Amy J. Knorpp,[a] Mark A. Newton,[a] Stefanie C. M. Mizuno,[b] Jie Zhu,[ab] Hiwote Mebrate,[b] Ana B. Pinar*[b] and Jeroen A. van Bokhoven*[ab]

The isothermal, low-temperature stepwise conversion of methane to methanol over copper-exchanged zeolites eliminates the time-consuming heating and cooling steps of the conventional high temperature activation approach. To better understand differences between the two approaches, a series of zeolites were screened, of which omega zeolite (MAZ) showed superior performance in both the isothermal and conventional approaches.

During the formation of fossil fuels over millions of years, a mixture of crude oil and methane often evolved together. Ultimately this leads to their co-extraction at petroleum extraction sites. For remote oil extraction sites, this methane can be more expensive to transport than its market value, and depending on local environmental legislation, the methane is reinjected, flared, or vented into the atmosphere.[1] Converting this stranded methane to different products (*i.e.* methanol) would not only mitigate waste but also allow for a nimbler hydrocarbon economy.[2] Methane is industrially converted to methanol using a catalytic steam reforming process to produce syngas in the first stage, followed by subsequent catalytic reaction to form methanol.[3] This route to methanol is too costly for implementation at dispersed methane sources. Alternatively, methane can be converted to methanol directly over copper-exchanged zeolites;[4] however, the development of this approach has not reached a level of industrial applicability, though it is advancing rapidly. Direct methane to methanol conversion is difficult, because the higher reactivity of methanol than methane sets a limit to the yield that can be obtained.[5–8] Currently, research in this area is at a transition point where scientific refocusing towards processes with more industrial feasibility are needed.[9]

One promising system using copper-exchanged zeolites is a stoichiometric stepwise ("chemical looping") procedure. The most widely studied stepwise procedure requires a high temperature activation step (723 K in O_2), a methane reaction step (473 K in CH_4), and finally a methanol extraction step (on-line with steam or off-line with water).[4,10–15] This conventional high temperature activation procedure has been extensively used to evaluate methanol yields achievable for a wide range of zeolite structures.[4,13,16,17] Within this stepwise procedure, much focus has been given to the nature of the active site with multiple different motifs proposed.[4,14,18–23] In spite of multiple proposed active sites, these works agree that high activation temperature (>623 K) in oxygen is required to form the active sites which store the activated oxygen that will selectively convert methane to methanol.[4,14,24] It was assumed that a high temperature activation was required until a low-temperature, isothermal, procedure was introduced where the activation and reaction are conducted at 473 K but with an elevated pressure of methane to boost the methanol yield.[25,26] The isothermal procedure suffers some penalty in regards to methanol yield in the case of Cu-mordenite (MOR),[25] but it has a clear advantage in terms of scale-up and ultimately, industrial implementation, because the isothermal procedure eliminates time-consuming heating and cooling between steps and cycles. Recent economic analysis of the direct conversion of methane to methanol has shown that (at least) a 50-fold improvement is needed for this process to be considered as industrially promising, and it highlighted research areas (methanol productivity, cost of material, and cycling time) to close this gap.[9] Given this, and the possible cycling time improvement, the isothermal procedure needs just as much or more attention paid to it as the conventional procedure, with the ultimate goal of rationally designing a zeolite that not only produces high methanol yields in the laboratory but can also be more easily implemented beyond the laboratory.

Unlike the conventional procedure, the isothermal route has not been as extensively studied. The first reports of the isothermal procedure evaluated three zeolite (Cu-Y, Cu-MOR, and Cu-ZSM-5).[25,26] Cu-MOR achieved the highest methanol yield of 55 μmol per gram-zeolite at 30 bar methane pressure.[25] This value is below regularly observed methanol yields (~160 μmol per gram-zeolite) for the conventional procedure.[27] Conversely for Cu-Y, more methanol was produced in the

[a] *Institute for Chemical and Bioengineering, ETH Zurich, Vladimir-Prelog-Weg 1, 8093 Zurich, Switzerland. E-mail: Jeroen.vanbokhoven@chem.ethz.ch*
[b] *Laboratory for Catalysis and Sustainable Chemistry, Paul Scherrer Institute, 5232 Villigen, Switzerland*

† Electronic supplementary information (ESI) available. See DOI: 10.1039/c9cc05659a

isothermal procedure than in the conventional procedure where it is virtually inactive;[25] and with further optimization of the reaction temperature, its methanol yield can be further increased.[28] This observation for Cu-Y is important because it shows that the structure–property relationships and active sites for the low-temperature, isothermal procedure are different than for the well-studied conventional procedure. This opens several questions for copper-exchanged zeolites and the isothermal procedure, that including: what is the active site?; are there patterns to structure–property relationships?; and, can higher methanol yields be achieved?

To better understand the similarity and differences between the low-temperature isothermal approach and the conventional high temperature activation approach, a series of zeolite frameworks were screened in both procedures. Zeolite samples were selected based on their varying performance in the conventional high temperature activation procedure. First zeolites with high activity in the conventional procedure were selected (CHA,[13,29] FER,[17] and MAZ[16,30]). Secondly the isothermal procedure allows an opportunity to examine more zeolite frameworks than the conventional procedure, due to the fact some zeolites are not stable at high activation temperatures. Without having to consider this limitation, we were able to select zeolites (MER, GIS, LTA, and OFF) based on the quantity of 8-membered rings in a unit cell.[31]

Additional samples of omega zeolite (MAZ) with varying performance in the conventional high temperature activation approach were selected. For the conventional procedure, the methanol yield for omega zeolite shows a dependence on the zeolite's morphology. The highest methanol yield was produced for the parent zeolite with large 1–2 μm bundle rods, and for a morphology of small spheres composed of 300 μm particles, the methanol yield was severely reduced.[32] The small spheres are denoted as MAZ-A and the larger bundled rods as MAZ-B. Additionally MAZ-B is inactive for methane conversion at low loadings of copper for the conventional procedure,[30] and this inactive MAZ-B sample was also tested for the isothermal conversion. Fig. 1 shows the zeolites analyzed and the chemical analysis as determined by atomic absorption spectroscopy as well as structural features of each zeolite.

There are no established "standard" conditions to screen different zeolites in the isothermal procedure. As such, we selected a scheme that used activation for 1 hour at 473 K in oxygen followed by a reaction in methane at 6 bar for 30 minutes. For comparison, the same samples were also tested under conventional high temperature activation conditions with activation for 1 hour in oxygen at 723 K and reaction at 1 bar methane for 30 minutes at 473 K. Methanol was extracted off-line and quantified by GC-FID. Fig. 1 shows the methanol yields for the screened zeolites under both the isothermal and conventional high temperature activation approaches.

A very wide variation in performance according to the applied method and the zeolite type employed results from this comparison. The zeolites (FER, CHA, MOR6.5, MOR10, and MAZ) that are active in the conventional procedure[4,13,14,27] all show conversion for the isothermal procedure, and the conventional procedure consistently outperforms the isothermal one. The highest methanol yield was observed for MAZ-B with 76 μmol-MeOH per gram-zeolite; however, whether omega zeolite (MAZ) is active is highly dependent on its synthesis and resulting morphology. For MAZ-A, the methanol yield was severely reduced with only 14 μmol-MeOH per gram-zeolite for the isothermal method. For low-copper containing MAZ-B, both the conventional and isothermal approaches yielded no methanol.

Conversely, samples LTA and OFF were inactive in the conventional high temperature activation procedure, but showed activity in the isothermal approach. OFF in particular yielded 21.8 μmol-methanol per gram-zeolite, which is comparable to the methanol yields observed for MOR10. Unlike the MOR framework, the OFF framework does not have 8-membered channels and yet produces methanol with yields equivalent to MOR6.5 under low-temperature, isothermal conditions. This indicates that such channels are not absolutely necessary for the isothermal procedure. What may be more important are the 8-membered side pockets or the larger 12-membered ring that are observed in both structures.[20]

No methanol was observed for MER, even though it has high density of 8-membered rings per unit cell, a structural feature previously concluded to be important for selective oxidation of methane.[16] For samples GIS and LTA degradation of the

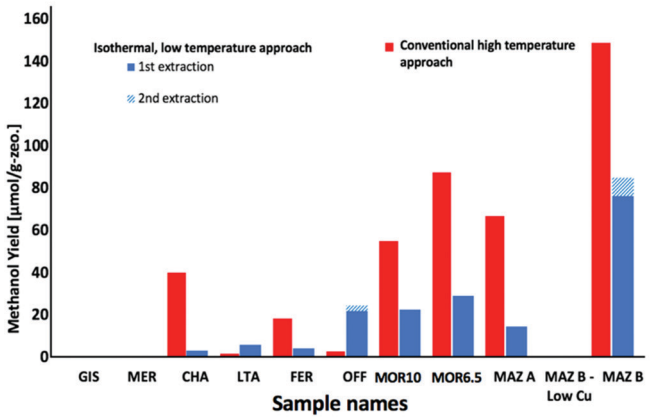

Sample Name	IZA Code	Si/Al	Cu wt.%	Pore size	
GIS	GIS	5.7	5.6	8 MR 8 MR	3.1 x 4.5 [100] 2.8 x 4.8 [010]
MER	MER	2.6	6.4	8 MR 8 MR 8 MR 8 MR	3.1 x 3.5 [100] 2.7 x 3.6 [010] 3.4 x 5.1 [001] 3.3 x 3.3 [001]
CHA	CHA	3.02	4.7	8 MR	3.8 x 3.8 ⊥ [001]
LTA	LTA	1.1	6.3	8 MR	4.1 x 4.1 [100]
FER	FER	15.3	1.6	10 MR 8 MR	4.2 x 5.4 [001] 3.5 x 4.8 [010]
OFF	OFF	4.3	4.0	12 MR 8 MR	6.7 x 6.8 [001] 3.6 x 4.9 ⊥ [001]
MOR10	MOR	9.7	4.7	12 MR 8 MR	6.5 x 7.0 [001] 2.6 x 5.7 [001]
MOR6.5	MOR	6.5	4.3		
MAZ A	MAZ	4.32	4.8	12 MR 8 MR	7.4 x 7.4 [001] 3.1 x 3.1 [001]
MAZ B-LowCu	MAZ	4.25	1.5		
MAZ B	MAZ	4.25	4.4		

Fig. 1 Methanol yields of various zeolites under isothermal conditions (6 bar methane) and conventional, high temperature activation conditions. Chemical analysis of exchanged zeolites tested for isothermal conversion of methane to methanol. Typical structure features, pore and channels sizes are included.[31]

framework was observed in the reacted material despite the low-temperature approach (Fig. S3, ESI†), which explains these zeolite poor performance.

Fig. 1 gives additional evidence that the structure–property relationships of this system are more complex than would be expected from considerations based purely on the pore and channel size. However, it appears to be generally true that if a structure is active in the conventional procedure, it is active when isothermally done, and factors such as the zeolite synthesis (and resulting morphology) will impact the two reactive procedures in similar manners. Conversely, if a structure is inactive in the conventional procedure, it may or may not be active in the isothermal procedure, and therefore screening of these frameworks is required.

MAZ-B showed the most promising conversion under isothermal conditions, and it was further investigated to better understand the isothermal procedure. To improve the methanol yields, the reaction was conducted under different pressures of methane (Fig. 2). For each pressure, the methanol was extracted offline, and multiple extractions were conducted until no methanol was observed by GC. Fig. 2 shows that MAZ-B and MOR10 follow a similar trend, with a sharp increase of the methanol yield at pressures between 1 and 6 bar, followed by levelling off of methanol yield at higher pressures. At 20 bar methane, a high methanol yield of 141 μmol-MeOH per gram-zeolite is achieved, which is nearly equivalent to the highest reported yields obtained from the conventional high temperature activation procedure for MAZ-B (150 μmol-MeOH per gram-zeolite) and Cu-MOR.[27] However, this yield is lower than reported for MAZ-B when both high temperature activation (723 K) and high pressures (36 bar) (200 μmol-MeOH per g-zeolite) are applied.[30] MAZ-B shows superior selectivity to MOR10, which results in MAZ-B's higher methanol yield. *In situ* FTIR (Fig. S6, ESI†) shows trace by-products of formate and carbon monoxide for MOR10, while for MAZ-B only trace carbon monoxide was observed. In general, the selectivity for the isothermal and the conventional procedures for both procedures are very high; however, the selectivity-conversion limit applies,[7] and the conversion is unquantifiably low.

When the reaction and activation steps are extended by four-fold in time, the methanol yield increases for the lower pressure of methane case (3 bar methane), but the methanol yield remains similar for the high pressure of 20 bar (Fig. 2). This may result from diffusion limitations at the lower temperature of operation that are overcome at higher methane pressures.

To understand the mechanism, the copper oxidation states were tracked by *in situ* Cu K-edge XANES throughout the oxygen activation and methane reaction. The high copper loaded MAZ-B has Cu(I) increasing rapidly between 1 and 6 bar and then subsequently levels off (Fig. 3). This pressure dependent trend is similar to methanol yield obtained in the reaction studies in Fig. 2 as well as previous *in situ* Cu K-edge XANES for isothermal Cu-MOR.[33] For the inactive low-copper loaded MAZ-B, the pressure has little effect on the formation of Cu(I) up to 6 bar with Cu(I) only being observed to form above 9 bar. At elevated pressures of 20 bar methane, this sample became active with a small amount of methanol (11 μmol-CH_3OH per gram-zeo.) extracted. Under high methane pressure, previously inactive copper in MAZ-B can become active. This was also observed for MAZ-B in the high activation temperature procedure.[30] The reason for this can only be speculated, but it is possible that improved diffusion, copper mobility[36] and the higher reduction potential may be responsible for this effect.

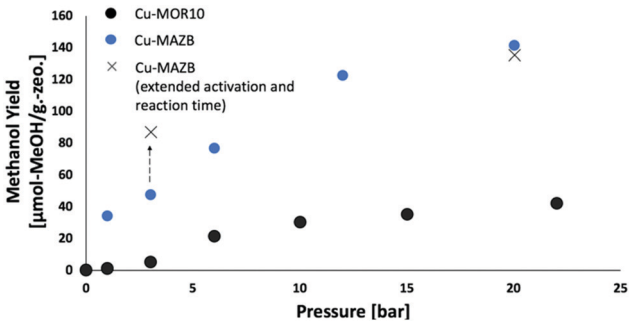

Fig. 2 Methanol yield as pressure increases for MAZB and MOR10. By extending the activation and reaction time, the methanol yield can be further increased if the reaction is conducted at low pressure.

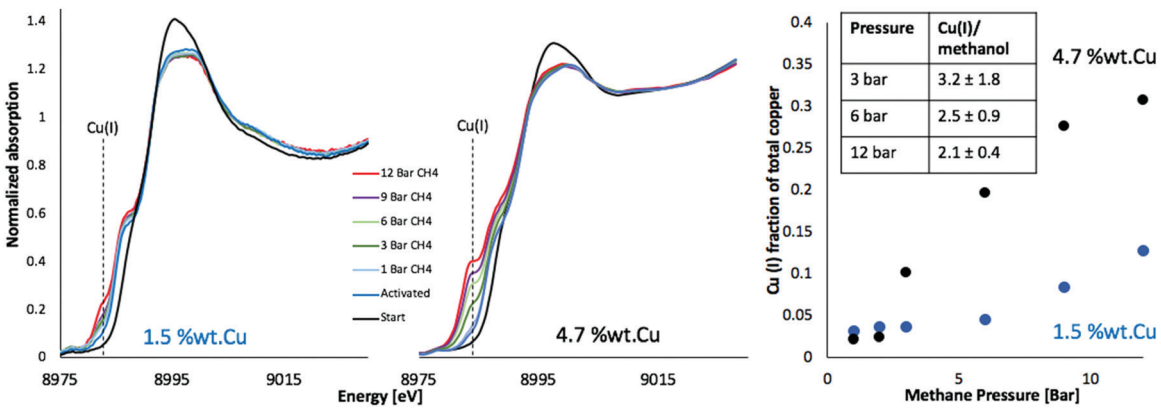

Pressure	Cu(I)/ methanol
3 bar	3.2 ± 1.8
6 bar	2.5 ± 0.9
12 bar	2.1 ± 0.4

Fig. 3 (left) *In situ* XAS at the Cu k-edge of low and high copper loaded MAZ-B as methane pressure increases during the reaction for the low temperature, isothermal protocol. (right) As the methane pressure increases, the higher copper loaded MAZ increases the formation of Cu(I) and levels off after 10 bar. Meanwhile, the low copper loaded sample, Cu(I) formation only occurs after 6 bar methane. Table shows the Cu(I) formed per methanol which indicates that it is a two-electron redox process at higher pressures.

The observed reduction of copper in Fig. 3 is consistent with a mechanism that involves a reduction–oxidation reaction with Cu(I) formation as fundamental to methanol formation. Increasing evidence has recently been derived to suggest that this is the dominant mechanism for conversion of methane to methanol under high activation temperature conditions,[27,30,34,35] and this mechanistic motif can be expanded to the isothermal process for Cu-MOR.[33] Fig. 3 shows the Cu(I) formed per methanol averaged over two separate in-situ Cu K-edge XAS experiments. As the pressure is increased, the results converge to approximately 2 Cu(I) formed per methanol. This indicates, at least mechanistically, the conversion of methane to methanol under the isothermal and conventional procedures are similar.[34] One may speculate that a precursor species to the generally assumed active site formed during the high-temperature activation is active in the case of isothermal and low temperature operation. However, water is not completely removed during activation of isothermal procedure, leaving partially water-poisoned active sites (Fig. S7, ESI†).

By expanding the database of zeolites tested for the conversion of methane to methanol under isothermal conditions, there is a significant overlap between zeolites (MAZ-B, MOR10, MOR6.5, CHA, and FER) that are active for both the conventional, high temperature and isothermal stepwise approaches to the selective activation of methane. Conversely, there are also zeolites (OFF) that are active in the isothermal but not the conventional procedure, showing that the structure–activity relationships observed in the conventional procedure cannot be absolutely applied to the isothermal procedure across all zeolite types. However, there is similarity between the two methods in respect to the mechanism, which is a 2-electron reduction process, and the selection of the parent zeolites morphology can affect the final yield.

Of the screened zeolites, MAZ-B showed superior performance, and by further investigating MAZ-B under low-temperature isothermal conditions, conversions of methane to methanol at levels that are commensurate with the conventional high temperature activation have been achieved. Furthermore, these levels come without the significant penalty of very large swings in temperature required by the latter method.

Conflicts of interest

There are no conflicts to declare.

Notes and references

1 T. A. Brzustowski, *Prog. Energy Combust. Sci.*, 1976, **2**, 129–141.
2 G. A. Olah, *Angew. Chem., Int. Ed.*, 2005, **44**, 2636–2639.
3 G. C. Chinchen, P. J. Denny, J. R. Jennings, K. C. Waugh and P. Group, *Appl. Catal.*, 1988, **36**, 1–65.
4 M. H. Groothaert, P. J. Smeets, B. F. Sels, P. A. Jacobs and R. A. Schoonheydt, *J. Am. Chem. Soc.*, 2005, **127**, 1394–1395.
5 J.-P. Lange, K. P. De Jong, J. Ansorge and P. J. A. Tijm, *Stud. Surf. Sci. Catal.*, 1997, **107**, 81–86.
6 M. Ahlquist, R. J. Nielsen, R. A. Periana and W. A. Goddard, *J. Am. Chem. Soc.*, 2009, **131**, 17110–17115.
7 M. Ravi, M. Ranocchiari and J. A. van Bokhoven, *Angew. Chem., Int. Ed.*, 2017, **56**, 16464–16483.
8 A. A. Latimer, A. Kakekhani, A. R. Kulkarni and J. K. Nørskov, *ACS Catal.*, 2018, **8**, 6894–6907.
9 J.-P. Lange, V. L. Sushkevich, A. J. Knorpp and J. A. van Bokhoven, *Ind. Eng. Chem. Res.*, 2019, **58**, 8674–8680.
10 N. V. Beznis, B. M. Weckhuysen and J. H. Bitter, *Catal. Lett.*, 2010, **138**, 14–22.
11 P. Vanelderen, R. G. Hadt, P. J. Smeets, E. I. Solomon, R. A. Schoonheydt and B. F. Sels, *J. Catal.*, 2011, **284**, 157–164.
12 E. M. Alayon, M. Nachtegaal, M. Ranocchiari and J. A. van Bokhoven, *Chem. Commun.*, 2012, **48**, 404–406.
13 M. J. Wulfers, S. Teketel, B. Ipek and R. F. Lobo, *Chem. Commun.*, 2015, **51**, 4447–4450.
14 S. Grundner, M. A. C. Markovits, G. Li, M. Tromp, E. A. Pidko, E. J. M. Hensen, A. Jentys, M. Sanchez-Sanchez and J. A. Lercher, *Nat. Commun.*, 2015, **6**, 7546.
15 S. E. Bozbag, E. M. C. Alayon, J. Pecháček, M. Nachtegaal, M. Ranocchiari and J. A. van Bokhoven, *Catal. Sci. Technol.*, 2016, **6**, 5011–5022.
16 M. B. Park, S. H. Ahn, A. Mansouri, M. Ranocchiari and J. A. van Bokhoven, *ChemCatChem*, 2017, **9**, 3705–3713.
17 D. Pappas, E. Borfecchia, M. Dyballa, K. A. Lomachenko, A. Martini, G. Berlier, B. Arstad, C. Lamberti, S. Bordiga, U. Olsbye, S. Svelle and P. Beato, *ChemCatChem*, 2019, **10**, 621–627.
18 J. S. Woertink, P. J. Smeets, M. H. Groothaert, M. A. Vance, B. F. Sels, R. A. Schoonheydt and E. I. Solomon, *Proc. Natl. Acad. Sci. U. S. A.*, 2009, **106**, 18908–18913.
19 P. Vanelderen, J. Vancauwenbergh, M. L. Tsai, R. G. Hadt, E. I. Solomon, R. A. Schoonheydt and B. F. Sels, *ChemPhysChem*, 2014, **15**, 91–99.
20 B. E. R. Snyder, P. Vanelderen, R. A. Schoonheydt, B. F. Sels and E. I. Solomon, *J. Am. Chem. Soc.*, 2018, **140**, 9236–9243.
21 V. L. Sushkevich, D. Palagin, M. Ranocchiari and J. A. van Bokhoven, *Science*, 2017, **356**, 523.
22 J. Meyet, K. Searles, M. A. Newton, M. Wörle, A. P. van Bavel, A. D. Horton, J. A. van Bokhoven and C. Coperet, *Angew. Chem., Int. Ed.*, 2019, **58**, 9841–9845.
23 D. Palagin, A. J. Knorpp, A. B. Pinar, M. Ranocchiari and J. A. van Bokhoven, *Nanoscale*, 2017, **9**, 1144–1153.
24 E. M. C. Alayon, M. Nachtegaal, A. Bodi, M. Ranocchiari and J. A. van Bokhoven, *Phys. Chem. Chem. Phys.*, 2015, **17**, 7681–7693.
25 P. Tomkins, A. Mansouri, S. E. Bozbag, F. Krumeich, M. B. Park, E. M. C. Alayon, M. Ranocchiari and J. A. van Bokhoven, *Angew. Chem., Int. Ed.*, 2016, **55**, 5557–5561.
26 P. Tomkins, M. Ranocchiari and J. A. van Bokhoven, *Acc. Chem. Res.*, 2017, **50**, 418–425.
27 D. K. Pappas, A. Martini, M. Dyballa, K. Kvande, S. Teketel, K. A. Lomachenko, R. Baran, P. Glatzel, B. Arstad, G. Berlier, C. Lamberti, S. Bordiga, U. Olsbye, S. Svelle, P. Beato and E. Borfecchia, *J. Am. Chem. Soc.*, 2018, **140**, 15270–15278.
28 V. L. Sushkevich and J. A. van Bokhoven, *ACS Catal.*, 2019, **9**, 6293–6304.
29 D. K. Pappas, E. Borfecchia, M. Dyballa, I. A. Pankin, K. A. Lomachenko, A. Martini, M. Signorile, S. Teketel, B. Arstad, G. Berlier, C. Lamberti, S. Bordiga, U. Olsbye, K. P. Lillerud, S. Svelle and P. Beato, *J. Am. Chem. Soc.*, 2017, **139**, 14961.
30 A. J. Knorpp, A. B. Pinar, M. Newton, V. Sushkevich and J. A. van Bokhoven, *ChemCatChem*, 2018, **10**, 5593–5596.
31 C. Baerlocher and L. B. McCusker, Database of Zeolite Structures, http://www.iza-structure.org/databases/.
32 A. J. Knorpp, M. A. Newton, V. L. Sushkevich, P. P. Zimmermann, A. B. Pinar and J. A. van Bokhoven, *Catal. Sci. Technol.*, 2019, **9**, 2806–2811.
33 A. J. Knorpp, M. A. Newton, A. B. Pinar and J. A. van Bokhoven, *Ind. Eng. Chem. Res.*, 2018, **57**, 12036–12039.
34 M. A. Newton, A. J. Knorpp, A. B. Pinar, V. L. Sushkevich, D. Palagin and J. A. van Bokhoven, *J. Am. Chem. Soc.*, 2018, **140**, 10090–10093.
35 G. Brezicki, J. D. Kammert, T. B. Gunnoe, C. Paolucci and R. J. Davis, *ACS Catal.*, 2019, **9**, 5308–5319.
36 C. Paolucci, I. Khurana, A. A. Parekh, S. Li, A. J. Shih, H. Li, J. R. Di Iorio, J. D. Albarracin-caballero, A. Yezerets, J. T. Miller, W. N. Delgass, F. H. Ribeiro, W. F. Schneider and R. Gounder, *Science*, 2017, **357**, 898–903.